Length Scale of Dynamic Heterogeneities at the Glass Transition Determined by Multidimensional Nuclear Magnetic Resonance

U. Tracht,[1] M. Wilhelm,[1] A. Heuer,[1] H. Feng,[1] K. Schmidt-Rohr,[2] and H. W. Spiess[1]
[1]*Max-Planck Institut für Polymerforschung, Postfach 3148, D-55021 Mainz, Germany*
[2]*Department of Polymer Science and Engineering, University of Massachusetts, Amherst, Massachusetts 01003*
(Received 18 December 1997)

We directly measure the equilibrium length scale of dynamic heterogeneities close to the glass transition by means of a new multidimensional NMR experiment. The spatial information is gained from a proton spin diffusion experiment combined with two 2D ^{13}C exchange sequences via appropriate back and forth transfer of magnetization between ^{13}C and ^{1}H spins. For poly(vinyl acetate) at 10 K above the glass transition we detected a length scale of 3 ± 1 nm. [S0031-9007(98)07244-5]

PACS numbers: 64.70.Pf, 76.60.–k

Supercooled amorphous systems exhibit a complex dynamic behavior (for a recent review, see Ref. [1], and references therein). For most glass-forming systems this results in highly nonexponential α relaxation. Recent experiments have demonstrated that the nonexponential time behavior is related to a superposition of relaxation processes, each characterized by an individual rate hence giving rise to the notion of *dynamic heterogeneities* [2–9], composed of *slow* and *fast* relaxators. Similar results have also been observed in polymer simulations [10]. Hence dynamic heterogeneities are an essential ingredient of the glass transition. Two characteristic properties of dynamic heterogeneities—time scale of fluctuations of rates and length scale ξ_{het} of temporary clusters of slow segments—are sketched in Fig. 1.

Information about the *time scale of fluctuations* within the distribution of reorientation rates has already been obtained from reduced four-dimensional solid state exchange NMR (*4D experiment*) [3,6,7,11] and from photobleaching [5]. Application of the 4D experiment to a variety of polymers [3,6,11] and low-molar glass formers [7] has clearly shown that the fluctuations within the heterogeneous rate distribution occur on the same time scale as the relaxation process itself.

The *length scale* ξ_{het} of the dynamic heterogeneities may be related to that of cooperatively rearranging regions (CRRs), first postulated by Adam and Gibbs [12,13]. It is reasonable to assume that ξ_{het} is an upper limit for the length scale of CRRs. As ξ_{het} is a fundamental parameter of the glass transition, several attempts to determine its value have been reported. Most approaches, however, involve perturbations of the system itself. Either the liquids are confined to pores [14–16] or probe molecules are added to the sample [17–19]. Information about the characteristic length scale is derived from the dependence of the α-relaxation properties on the size of the confining structure or the probe molecule. Interpretation of these experiments has to take into account that, e.g., the relaxation in pores strongly depends on the surface properties of the host [15,16] and that large probe molecules may change the local dynamics. Within the model of cooperatively rearranging regions Donth has estimated the length scale of these regions to be close to 2 nm [13,20].

Obviously it is desirable to have a method which allows one to directly measure the length scale of dynamic heterogeneities of the glass transition in a *nonperturbative* way. In this Letter we present a new experiment (*4D-CP experiment*) achieving this goal. It is an extension of our previous 4D exchange ^{13}C-NMR experiment [3,6,11], where slow segments are selected and fluctuation of their rates during a waiting time t_{m2} is monitored; see Fig. 1 of Ref. [6]. We now combine this 4D experiment with ^{1}H spin diffusion during t_{m2}, providing spatial information. The paper is organized as follows: First, we give the general idea of our new approach and show how these ideas are realized experimentally; then experimental data are presented for poly(vinyl acetate) (PVAc) slightly above the glass transition temperature T_g. Finally, a quantitative analysis of these data is performed.

In Fig. 2 the idea of the 4D-CP experiment as well as the original 4D experiment is described on the basis of a bimodal distribution with rates k_{slow} and k_{fast} [Fig. 2(a)].

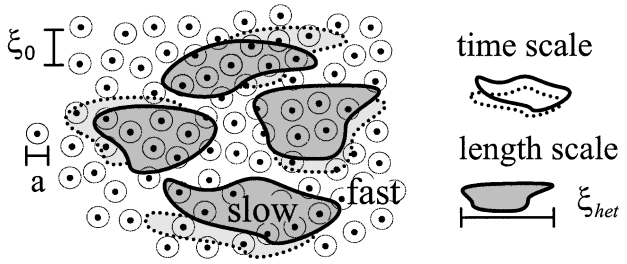

FIG. 1. Sketch of the temporal fluctuations as well as the length scale of dynamic heterogeneities. The temporal fluctuations are related to a time scale in the sense that a specified segment may switch between a fast and a slow state. The positions of the individual ^{13}C spins are indicated. The circles around them indicate the region of the proton bath from which magnetization can be transferred back to the ^{13}C spins. We note that it is also possible that the regions of slow segments display a continuous, more fractal structure.

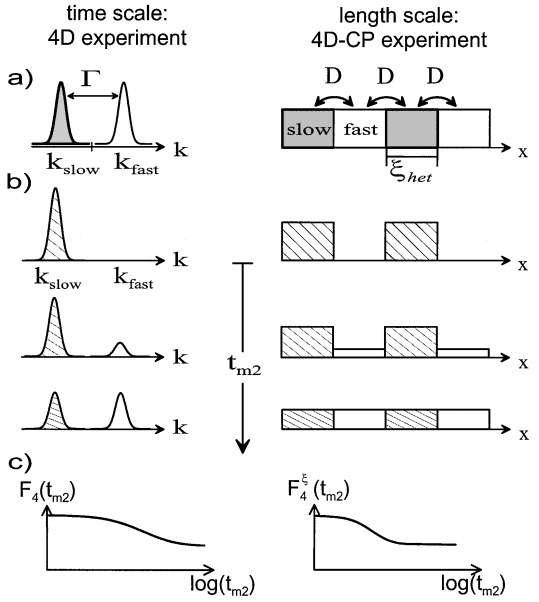

FIG. 2. Schematic description of the 4D and the 4D-CP experiment, determining the time and length scale of dynamic heterogeneities, respectively. In (a) simple models are displayed, for (left) exchange processes with rate Γ in a bimodal distribution with rates $k_{\rm slow}$ and $k_{\rm fast}$ and (right) spin diffusion in a 1D array of slow and fast regions with length scale $\xi_{\rm het}$, neglecting exchange processes. In (b) it is shown how the magnetization, initially, i.e., for $t_{m2} = 0$, connected with the slow segments, equilibrates with increasing waiting time t_{m2} due to exchange process or spin diffusion, respectively. The magnetization, remaining on the slow component, is indicated by the shaded areas. The dependence of this magnetization on t_{m2} is displayed in (c). After normalization to one these curves are denoted $F_4(t_{m2})$ and $F_4^{\xi}(t_{m2})$, respectively. Their t_{m2} dependence allows one to estimate the exchange rate Γ or the length scale $\xi_{\rm het}$, respectively.

The first step of the 4D as well as the 4D-CP experiment is to selectively magnetize the ^{13}C spins, related to slow segments and to monitor the subsequent equilibration of magnetization [Fig. 2(b)]. One may distinguish two equilibration processes in time and space, respectively. In the 4D experiment one observes equilibration at a fixed ^{13}C nucleus due to exchange processes rendering fast segments slow and vice versa. In this way magnetization is more and more connected also to fast segments and the observed magnetization, denoted $F_4(t_{m2})$, decreases with time until equilibration [Fig. 2(c)]. In contrast, in the 4D-CP experiment one additionally enables spin diffusion during the variable waiting time t_{m2} (see below for more details). In this way magnetization can be transported to more mobile regions. Here the final magnetization on the slow segments is denoted $F_4^{\xi}(t_{m2})$ containing information about $\xi_{\rm het}$ [Fig. 2(c)]. Of course, $F_4^{\xi}(t_{m2})$ is also sensitive to exchange processes (see also below). Formally, $F_4(t_{m2})$ can be viewed as a four-time correlation function (see Ref. [6] for details) and in analogy $F_4^{\xi}(t_{m2})$ as a four time-space correlation function.

The 4D-CP experiment, as sketched above, contains two important ingredients: (i) enhancement of spin diffusion and (ii) selection and detection of slow segments before and after the waiting time t_{m2}. The enhancement of spin diffusion during the waiting time t_{m2} is achieved via transfer of ^{13}C magnetization to the proton bath. Whereas direct ^{13}C-^{13}C spin diffusion is negligible, the ^{1}H spin diffusion is sufficiently fast for the present purpose. The transfer of magnetization is achieved via cross polarization (CP) [11]. In analogy to the 4D experiment the selection and detection process is achieved by using 2D-echo filters with filter time t_{m0} [6]. The desired magnetization, i.e., $F_4^{\xi}(t_{m2})$, corresponds to the height of the final echo. The 4D-CP experiment is sketched in Fig. 3.

The experiments were performed on PVAc, 40% ^{13}C enriched at the carbonyl group which serves as a sensor of structural relaxation [21]. NMR echoes were recorded at $T = 315$ K $= T_g^{\rm DSC} + 10$ K on a Bruker MSL 300 spectrometer operating at ^{1}H and ^{13}C resonance frequencies of 300.13 and 75.47 MHz, respectively. All CP times were set to 0.8 ms and the recycle delay to 3 s. The evolution time of the 2D-echo filters [6] was $t_p = 200$ μs unless specified otherwise. CP times were optimized to exclude equilibration of magnetization during the CP pulses while retaining most of the signal intensity. Because of the low signal-to-noise (S/N) ratio of this experiment up to 10 000 accumulations were necessary for a single data point. The overall relaxation of the sample was determined by a 2D-echo experiment fitted to a stretched exponential $\exp[-(t_m/\tau_0)^{\beta}]$ yielding $\tau_0 = 16$ ms and $\beta = 0.45$. The filter times t_{m0} of the 4D and 4D-CP experiments were chosen to be 3.5 ms. In this way about 60% of the overall rate distribution were selected.

The resulting curve $F_4(t_{m2})$ is displayed in Fig. 4(a). In Fig. 4(b) the results of the 4D-CP experiments are displayed. First we note that the decay of F_4^{ξ} occurs on much shorter time scales than for F_4. Hence exchange processes can be neglected for the interpretation of F_4^{ξ} and the observed decay is exclusively related to spin diffusion processes, hence containing information about $\xi_{\rm het}$. For a quantitative interpretation we have to take into account that not all ^{1}H magnetization can be transferred back to ^{13}C after t_{m2}. The regions whose ^{1}H

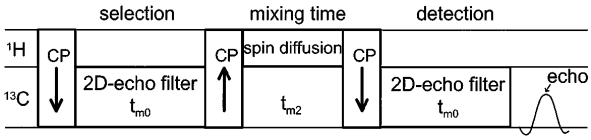

FIG. 3. Schematic representation of the 4D-CP experiment. The final echo height as a function of t_{m2} corresponds to $F_4^{\xi}(t_{m2})$. The transfer of magnetization to the proton bath via CP is essential to enable efficient spin diffusion between regions of slow and fast segments. Without CP this experiment reduces to the original 4D experiment; see Fig. 2 of Ref. [6].

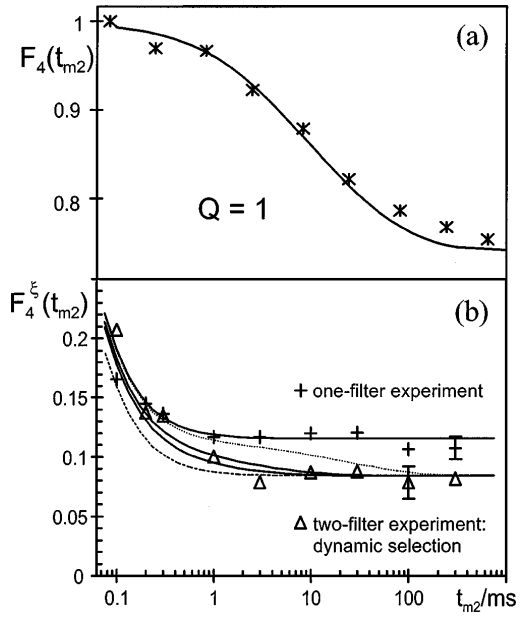

FIG. 4. Experimental curves F_4 of the (a) 4D experiment normalized to $F_4(t_{m2} = 0) = 1$ as well as the theoretical curve for a rate memory parameter $Q = 1$ as defined in [6,22] and (b) F_4^{ξ} (4D-CP experiment) for one and two filters. Experimental errors are indicated for the data points with largest t_{m2} only. The curves in (b) result from model calculations, described in the text. Upper solid line: equilibration on the length scale ξ_0, lower solid lines: length scales ξ_{het} of 2 and 4 nm, respectively, dashed line: statistical distribution ($\xi_{\text{het}} = 0$), and dotted line: upper limit of experimentally accessible length scales corresponding to $\xi_{\text{het}} \approx 20$ nm.

magnetization is lost is sketched in Fig. 1 as being outside the circles of size a surrounding each ^{13}C. Clearly this loss of magnetization is related to the average distance ξ_0 between the ^{13}C spins, being 0.7 nm in our case of 40% ^{13}C enrichment. Diffusion on both length scales ξ_0 and ξ_{het} can be separated by measuring F_4^{ξ} with and without 2D-echo filters. On a qualitative level comparison of both experiments contains information about the relative values of ξ_{het} and ξ_0 with the internal standard ξ_0 known from the sample preparation. Direct comparison of two data sets requires that they are recorded under similar conditions, in particular, applying the same number of pulses. Therefore, in the reference experiment the first 2D-echo filter was retained and the pulse delay t_p of the second was set to 1 μs in order to suppress the filter effect [6]. This experiment is denoted a one-filter experiment as compared to the two-filter experiment with both selection and detection of slow segments.

Note that the plateau values of both curves are well defined. Their ratio is determined by the known fraction of selected slow segments. The fact that the S/N ratio of the F_4^{ξ} is only a few percent of that of F_4 is partly due to the finite magnetization transfer efficiency and partly to the loss of magnetization to the proton bath. The absolute plateau values in Fig. 4(b) have been obtained by assuming a magnetization transfer efficiency of about 40%. Anyhow, as will be discussed below, the determination of ξ_{het} is insensitive to this normalization.

Neglecting complications due to magnetization transfer effects the signal $F_4^{\xi}(t_{m2})$ is given by

$$F_4^{\xi}(t_{m2}) \propto (4\pi D t_{m2})^{-3/2} \int d\vec{r}\, \exp(-\vec{r}^{\,2}/4Dt_{m2})\bar{\rho}(\vec{r})\,. \tag{1}$$

Equation (1) expresses the propagation of magnetization via spin diffusion with diffusion constant D starting from an arbitrarily selected slow ^{13}C spin at $\vec{r} = 0$. The term $\bar{\rho}(\vec{r})$ denotes the average density of slow ^{13}C spins at position $\vec{r}$ relative to the specified slow ^{13}C spin. This term takes into account that after spin diffusion during t_{m2} only magnetization related to slow spins is again selected and finally measured. A clustering of slow molecules gives rise to a nontrivial behavior of $\bar{\rho}(\vec{r})$. The simplest approach is to write

$$\bar{\rho}(\vec{r}) = \delta(\vec{r}) + (1/\xi_0^3)[p + (1 - p)\exp(-2|\vec{r}|/\xi_{\text{het}})], \tag{2}$$

thereby introducing the correlation length ξ_{het}. The delta function denotes the self-correlation term. Furthermore, the second term expresses that very close to the specified ^{13}C spin it is very probable that another ^{13}C spin is also slow whereas for distances much longer than ξ_{het} a constant probability p is reached. Since F_4 and the ratio of the two-filter to the one-filter data reach the same equilibrium value one can identify $p = F_4(\infty) = 0.72$. Of course, without selection, i.e., in the one-filter experiment, one has $p = 1$. The above expression neglects effects due to details of the magnetization transfer and the presence of exchange processes as discussed above. However, this can be taken into account by considering that (i) after the CP to protons the magnetization is distributed around the individual ^{13}C spins with a Gaussian with variance a^2 (see Fig. 1), (ii) the back transfer of magnetization of a proton at $\vec{r}_H$ to a ^{13}C spin at $\vec{r}_C$ is proportional to $\exp[-(\vec{r}_H - \vec{r}_C)^2/2a^2]$, and (iii) the presence of a cluster of slow segments around a tagged segment disappears by exchange processes, expressed by F_4. For our experimental data the exchange processes can be neglected on the time scale of the relevant spin diffusion process. Adjustable parameters are D, a, and ξ_{het}. D and a are obtained from the decay time and the final plateau value of the one-filter data, respectively. Using these parameters one can extract the value of ξ_{het} from the decay time of the two-filter experiment.

In Fig. 4(b) the fitted curves for the one-filter and two-filter data are displayed, the latter also for different values of ξ_{het}. The experimental data are compatible with values of ξ_{het} between 2 and 4 nm. For larger values the plateau would not be reached for $t_{m2} = 3$ ms; for

much smaller values of ξ_{het} the plateau value should be already reached for times as small as 0.3 ms, both in contrast to the experimental data. The adjustable parameters are $D = 0.42\ \text{nm}^2/\text{ms}$ and $a = 0.1$ nm. The value of D is a factor of about 1.5–2 smaller than typical ^{1}H spin diffusion constants [11], which can be attributed to the contribution of spin diffusion during the CP times with a scaled dipolar coupling [23]. The small value of a/ξ_0 reflects the significant loss of magnetization to the proton bath. We checked that the assumption of lower CP efficiencies going together with higher plateau values (between 12%/8% as in Fig. 4 and 58%/42% for the one- and the two-filter experiments, respectively) changes only the parameters a and D but not ξ_{het} because the experiment primarily determines the ratio ξ_{het}/ξ_0.

The main achievement of our new experiment is that we were able to determine a length scale of the glass transition, related to the size of dynamic heterogeneities. Slow segments are clearly clustered together as ξ_{het} is significantly larger than the diameter of a repeat unit. In contrast to previous related attempts [2,14–19] our approach, for the first time, directly measures length and time scales of dynamic heterogeneities independently. Moreover, the results can be expressed in terms of an equilibrium observable. This has the advantage that (i) the length scale has a well-defined meaning, (ii) one does not have to worry about the effect of external perturbations, and (iii) via Eqs. (1) and (2) the present approach can be directly translated to computer simulations. The fact that our results are compatible with estimates from other experiments in glass-forming systems [14] and the results by Donth *et al.* [13,20] show that the dynamic heterogeneities seem to be closely related to CRRs. However, a precise relation between CRRs and dynamic heterogeneities has still to be formulated. Length scales, obtained by the experiments mentioned before, are often of the same order [14,17] but also much larger, e.g., [16], as well as smaller values, e.g., [15], are found. This underlines that it is important to use well-defined concepts to *define* and *measure* a length scale at the glass transition. In principle one might study ξ_{het} as a function of temperature. However, the results by Donth *et al.* [20] indicate that no significant temperature dependence is to be expected within the range of temperatures accessible to the NMR experiments.

In summary, the length scale of dynamic heterogeneities in supercooled PVAc has been determined in a *nonperturbative* experiment combining ^{13}C multidimensional exchange NMR and ^{1}H spin diffusion techniques. Clusters of slow segments with diameter of $\xi_{\text{het}} = 3 \pm 1$ nm have been identified. Together with the previous determination of the lifetime of dynamic heterogeneities we have obtained detailed and model-free information about the complex dynamics on intermediate length scales near the glass transition.

We thank H. Zimmermann for providing us with the ^{13}C enriched PVAc. This work was partly supported by the Deutsche Forschungsgemeinschaft (SFB 262). U. T. gratefully acknowledges financial support from the BMBF and the "Stiftung Stipendien-Fonds des Verbandes der Chemischen Industrie."

[1] M. D. Ediger, C. A. Angell, and S. R. Nagel, J. Phys. Chem. **100**, 13 200 (1996).
[2] K. L. Li, A. A. Jones, P. T. Inglefield, and A. D. English, Macromolecules **22**, 4198 (1989).
[3] K. Schmidt-Rohr and H. W. Spiess, Phys. Rev. Lett. **66**, 3020 (1991).
[4] C. T. Moynihan and J. Schroeder, J. Non-Cryst. Solids **160**, 52 (1993).
[5] M. T. Cicerone and M. D. Ediger, J. Chem. Phys. **103**, 5684 (1995).
[6] A. Heuer, M. Wilhelm, H. Zimmermann, and H. W. Spiess, Phys. Rev. Lett. **75**, 2851 (1995).
[7] R. Böhmer, G. Hinze, G. Diezemann, B. Geil, and H. Sillescu, Europhys. Lett. **36**, 55 (1996).
[8] B. Schiener, R. Böhmer, A. Loidl, and R. V. Chamberlin, Science **274**, 752 (1996).
[9] R. Richert, J. Phys. Chem. B **101**, 6323 (1997).
[10] A. Heuer and K. Okun, J. Chem. Phys. **106**, 6176 (1997).
[11] K. Schmidt-Rohr and H. W. Spiess, *Multidimensional Solid-State NMR and Polymers* (Academic Press, London, 1994).
[12] G. Adam and J. H. Gibbs, J. Chem. Phys. **43**, 139 (1965).
[13] E. Donth, J. Non-Cryst. Solids **53**, 325 (1982).
[14] R. Richert, Phys. Rev. B **54**, 15 762 (1996).
[15] M. Arndt, R. Stannarius, W. Gorbatschow, and F. Kremer, Phys. Rev. E **54**, 5377 (1996).
[16] M. Arndt, R. Stannarius, H. Groothues, E. Hempel, and F. Kremer, Phys. Rev. Lett. **79**, 2077 (1997).
[17] M. T. Cicerone, F. R. Blackburn, and M. D. Ediger, J. Chem. Phys. **102**, 471 (1995).
[18] M. T. Cicerone, F. R. Blackburn, and M. D. Ediger, Macromolecules **28**, 8224 (1995).
[19] A. K. Rizos and K. L. Ngai, Mater. Res. Soc. Symp. Proc. **455**, 141 (1997).
[20] J. Korus, E. Hempel, M. Beiner, S. Kahle, and E. Donth, Acta Polym. **48**, 369 (1997).
[21] K. Zemke, K. Schmidt-Rohr, and H. W. Spiess, Acta Polym. **45**, 148 (1994).
[22] A. Heuer, Phys. Rev. E **56**, 730 (1997).
[23] S. Zhang, B. H. Meier, and R. R. Ernst, Solid State Nucl. Magn. Reson. **1**, 313 (1992).